NASA TECHNICAL TRANSLATION NASA TT F-13,938

EXPERIMENTAL STUDY ON THE GROUND EFFECT OF A MODEL HELICOPTER ROTOR IN HOVERING

Jiro Koo and Toichi Oka

Translation of Report NAL-TR-113, National Aerospace Laboratory, Tokyo, 1966, 19 pages

NATIONAL AERONAUTICS AND SPACE ADMINISTRATION
WASHINGTON, D.C. 20546 DECEMBER 1971

EXPERIMENTAL STUDY ON THE GROUND EFFECT CF A MODEL HELICOPTER ROTOR IN HOVERING

[Article* by Jiro Koo** and Toichi Oka**; Tokyo, National Aerospace Laboratory, Japanese, Report NAL-TR-113, 1966, 19 pages]

[English Abstract]

Aerodynamic characteristics of a model helicopter rotor hovering in the ground effect have been experimentally investigated. Although a number of papers have been written on this subject (ref. 1-4, etc.), there still remains much to be explored about the rotor in the unsteady condition.

We conducted two kinds of experiments i. e., (1) measurements of the thrust, torque and induced velocity of the hovering rotor in the ground effect and (2) flow visualizations around the hovering rotor in the ground effect by the use of tuft.

The qualitative results obtained are as follows.

(1) When a hovering rotor in higher pitch angle gets near to the ground ($H < 1/4D$), there is a saturation in the thrust increase from the ground effect according to the blade stall.

If a rotor is operated in lower pitch angle, the torque for the con-

---

* Received 6 August, 1966.
** Flight Experiment Department.

stant revolution increases gradually with the approach to the ground, however, in the next stage (i. e. $H < 1/4D$) it begins to decrease by up-wash which makes the lift vector incline forward.

(2) It appears from flow observations that the periodical fluctuation of interference flow between down-wash and up-wash may introduce the unsteady phenomena of a hovering helicopter in the ground effect.

1. Introduction

Generally speaking, when any type of an airplane flies close to the ground, there exists a so called "ground effect" which causes an increase or a decrease in the lift and a variation in the equilibrium moment. For helicopters, the ground effect usually assists in overweight conditions and in taking off from high altitude locations, and it is playing an important part in operations. Many studies have been conducted on this effect, but most of them did not consider unsteady aerodynamic conditions. However, the unstable phenomena actually occur only when the ground effect is produced by a helicopter hovering near the ground. It is also possible that when the rotor approaches the ground and the pitch angle of the blades is increased, a stall condition occurs. Taking this unsteady condition into consideration and using a model helicopter rotor, we measured the variations in the thrust and torque accompanying the variations in the altitude relative to the ground and the variations in the induced velocity distribution during hovering. At the same time we investigated the stall condition using silk string tufts attached to the upper surface of the blades. We also made a frame for air current observations by binding many

silk strings to a wire net. We observed the direction of the air flow around the rotor by placing the frame under it. Flight experiments were also conducted on the aspects of control of a helicopter hovering near the ground, and the effect of these phenomena on operations was investigated.

2. Symbols

b : number of blades

c : chord length of blade wing

D : diameter of rotor

H : elevation above ground (at center of rotor hub)

Q : torque

R : radius of rotor

r : distance from rotor axis

T : thrust

v_i : induced velocity

$\bar{v}$: mean of induced velocities (equation 2)

y : distance from center of rotor hub

$C_Q = Q/\rho\pi R^5\Omega^2$: torque coefficient

C_{Q_0} : profile torque coefficient (equation 1)

$C_T = T/\rho\pi R^4\Omega^2$: thrust coefficient

θ_0 : blade pitch angle at base of wing

$\theta_{0.75}$: blade pitch angle at 0.75R

Ω : angular velocity of rotor

ρ : density of air

$\sigma = bc/\pi R$: solidity

∞ : value at large elevations above the ground

3. Experimental Apparatus

Figure 1 shows the outline of the experimental apparatus. In order to make it easy to establish the interval between the rotor and the ground, that is, the elevation above ground, we erected the ground board in a vertical position, turned the model rotor sideways, and placed it on a cart, so that it was possible to move it along tracks to a position corresponding to any elevation. In order to prevent any interference to the down-wash of the rotor from surrounding walls and delicate breezes, the experiments were conducted at the center of the airplane structure laboratory (40m x 40m x 18m) of the Azabu Airport Branch.

3.1 Model Rotor

Table 1 lists each part of the rotor used in the experiments. With three aluminum alloy blades, freely moving flapping and lagging hinges, and a half fixed feathering hinge, pitch angles (θ_0) can be set every 2.5° when the 18% cord of the blade is the axis. We don't have a cycling pitch structure.

The rotor, operating through a torsion tube to measure torque and four plate springs to measure thrust, has a mechanism for separating and extracting the torque and thrust without interference using strain gauges stretched across them.

An 800W DC servomotor is used to operate the rotor. Throughout these experiments we set the revolution of the rotor at about 1030 rpm. A pulse was produced by a microswitch for every revolution of the rotor hub, and it was recorded and read on an oscillograph.

3.2 Ground Board and Air Flow Observation Apparatus

The ground board consists of plywood and acrylic resin boards

covering a 4 m high and 5 m wide wooden frame. It was set vertically, about 30 cm from the bed, and it was fixed parallel to the plane of revolution of the rotor. For the elevation above ground (H) in the experiments, we measured the distance between the center of the rotor hub and the ground board.

The interference conditions of the air flow can be observed from below the rotor through the acrylic resin board (1 m x 1 m) which was inserted near the center of the ground board. Using smoke tubes and dandelion seeds, we observed the conditions in this way when the rotor neared the ground. Furthermore, in order to investigate in detail the range of up-wash phenomena which can be observed within certain elevations, we made a wire net which is shown in Figure 2. This net consists of wire stretched at 5 cm intervals and silk strings attached to the wire. In order to determine at one glance whether the air flow is down-wash or up-wash, we illuminated the ground side of the wire with green light and the rotor side with orange light. The white silk strings became colored depending on their direction.

In order to observe the stalling condition of the blades, their upper surface was covered with about 1 cm long tufts. The microswitch, which records the number of revolutions, was synchronized with a stroboscope, which was observed and filmed. In order to aid observation in these experiments, we covered the ground board with black velvet. The effect of these tufts and the velvet on the measured values (thrust, torque) is practically unnoticeable.

4. Measured Values

4.1 Aerodynamic Characteristics of Model Rotor (No Ground Effect)

We measured the variations in the thrust (T) and torque (Q) with the changes in the blade pitch angle (θ_0) when the rotor hovered at a location without ground effect. Table 2 shows the relationship between the measured values of the blade pitch angle at the base of the wing (θ_0), effective pitch angle ($\theta_{0.75}$), and thrust coefficient without ground effect (C_T) and the values of the blade loading coefficient (C_T/σ) which is often used in ground effect analysis. Figure 3 shows these results with polar curves of C_T and C_Q. The dotted line in the figure indicates the profile torque coefficient (C_{Q_0}), which we calculated from the measured values of C_T and C_Q using equation 1 below.

$$C_T = T/\rho\pi R^4\Omega^2$$
$$C_Q = Q/\rho\pi R^5\Omega^2$$
$$C_{Q_0} = C_{Q\infty} - C_{T\infty}(\bar{v}/R\Omega) \qquad (1)$$

Using equation 2 below, we determined $\bar{v}$, the mean of the induced velocities, from the measured values of the thrust.

$$\bar{v} = \sqrt{T/2\rho\pi R^2}$$
$$= \Omega R\sqrt{C_T/2} \qquad (2)$$

At this time we measured the distribution of the perpendicular components of the induced velocity (v_i) with a pitot tube and a slope manometer. Figure 4 shows an example when the pitch angle (θ_0) is 15°. The parameter (y) in the figure is the distance between the tip of the pitot tube and the central surface of the rotor, and the figure shows that the downwash concentrates as the distance from the rotor surface increases. The straight line indicates the value of the induced velocity averaged over the whole surface of the rotor, measured at y = 100 mm = 0.091D, and the dotted

line indicates the value ($\bar{v}$) calculated from the thrust using equation 2. The value measured with the pitot tube is different from the value calculated from the thrust probably because of the difficulty of measuring small, swirling wind velocities with a pitot tube and because of the effects of the air flow at the edges of the rotor and near the hub.

4.2 Aerodynamic Variations Due to Ground Effect

Figures 5 and 6 show that the thrust and torque of a rotor hovering at a constant rate of revolution change as the rotor approaches the ground. The T/T_∞ and Q/Q_∞ values on the vertical axis are dimensionless quantities of the thrust and torque divided by their values when there is no ground effect. In Figure 5, when the pitch angle (θ_0) is over 12.5° and the rotor approaches the ground, stalling starts from the base of the blade and the increasing curve of the thrust levels off. We verified this condition in the air flow experiment mentioned later. The dotted line in the figure shows the predicted value of the thrust when the lack of stalling is assumed. In Figure 6, when the pitch angle is small, the torque first increases then decreases as the rotor nears the ground ($H/D<0.25$). It is possible that this is because the air flow around the rotor became the same as during descent, the effective joining angle increased from the up-wash of the central part, the lift acting there tilted forward, and a condition similar to autorotation occured.

Figure 7 shows how much the variation in thrust and torque caused by the ground effect assists the power by making the elevation parameter of the C_T-C_Q curve the same as in Figure 3. From this figure we can see that the power necessary to obtain the same thrust decreases from the ground effect. In Figures 5 and 7, the increase in C_T with the loading coefficient (C_T/σ)

caused by the ground effect is less than the theoretical value.[1,3] This is because of the structure of the model; probably because of the larger hub. Also, we cannot neglect the effect of corkscrewing. From now on, it will be necessary to investigate how the ground effect is influenced by corkscrewing, by the size of the model, and by the solidity. However, we think the results of our experiments are analytically correct.

4.3 Distribution of Induced Velocities

With a pitot tube and inclined manometer, we measured the variation in the distribution of the induced velocities as the rotor neared the ground. This is shown in Figure 4. It is difficult to measure the perpendicular components accurately with a pitot tube because the direction of the air flow varies greatly near the ground, at the edge of the wings, and at the central part of the up-wash, but we concentrated on obtaining analytic data this way because no other adequate measuring apparatus are available.

We performed experiments with the blade pitch angle at 10°, 12.5°, 15°, and 20°, but because we could find no large differences in the variation of the distribution, we will describe the conditions when θ_0 is 15°. This is equivalent to a regular helicopter during hovering.

Figures 8, 9, and 10 show that the distribution of induced velocities varies according to the elevation (H) of the rotor hub when the distance (y) between the plane of revolution and the pitot tube is 100 mm, 300 mm, and 500 mm respectively. As the rotor nears the ground, the greater component of the induced velocity moves to the outside, its width decreases, and it forms a tube shaped air curtain. Also, there is an up-wash at the ground and near the part surrounded by this curtain which

moves with time toward the rotor hub. The static pressure inside this air curtain seemed to become very high when the rotor approached the ground.[2]

5. Unstable Air Flow Phenomena

5.1 Blade Stall

We observed a revolving blade covered with silk string tufts by shining a stroboscope on it from above, and we investigated the applicable range of the blade pitch angle (θ_o) and the effects of corkscrewing. Figure 11 shows a photograph of this; most wings stalled only when θ_o was 20°. On the other hand, no stalling could be seen at θ_o=15° and θ_o=10°, although there was a little flow outward near the base of the wing.

The results of the measurements mentioned in the previous paragraph showed that the thrust saturated instead of increasing when and the blade approached the ground. In order to verify the hypothesis that stalling is the reason for this, we tried to bring the rotor near the ground board. Figures 12 and 13 are examples of photographs. As shown in Figure 12, where θ_o=15° and the rotor is near the ground (H = 0.25D), the angle of elevation increases and pulls away near the base of the wings when the pitch angle is large. At θ_o=10° (Figure 13), the flow outward becomes slightly stronger, and little stall occurs. It is clear from comparing Figures 12 and 13 that the stall occurs when the rotor operating with a large pitch angle approaches the ground.

5.2 Air Flow Around the Rotor

Burning a smoke candle at the upper surface of the rotor, we observed the condition of the air flow from the acrylic resin window at the center of the ground board and from the side of the rotor. Figure 14

shows a photograph taken from the side. We found that a part of the up-wash starts to swirl when the rotor approaches the ground and the air flow under the rotor moves with time during hovering at low elevations.

In order to investigate this in more detail, we bound tufts to a wire net as shown in Figure 2 and placed it 100 mm under the rotor. Figure 15 shows a photograph which was taken at $\theta_0=15°$ and $H=0.5D$. The part at the center where the strings look frizzled is the up-wash region. In order to observe this phenomenon clearly, we illuminated the tufts blown toward the ground and those blown toward the rotor with different color lights and made a color movie. Figure 16 shows sketches of 0.5 second intervals. It can be seen from the figure that the up-wash region swirls periodically in the direction of the revolution together with the region where the sideways flow is strong and its width changes with time. The width of this region and its speed of movement increase as the pitch angle gets larger and the rotor nears the ground. It is assumed that this movement of the up-wash effects the tail rotor, stabilizing fins, and body and makes the helicopter unstable during hovering.

5.3 Flight Experiments on Instability

Using flight experiments on a small helicopter, we confirmed that the stability deteriorates when a hovering helicopter approaches the ground.

Taking the hovering elevation as the parameter, we measured the movements of the pilot operated control stick when the helicopter hovered over one point for a given length of time. The results are shown in Figure 17. The value of the hovering elevation divided by the rotor diameter is shown on the horizontal axis, and the area covered by the loci of the

movements of the tip of the control stick is shown on the vertical axis.

The rapid increase of this area as the helicopter approached the ground seems to prove that the instaoility increases for the reasons described in the previous paragraph.

6. Conclusions

We arrived at the following analytical conclusions based on our series of experiments on the various phenomena produced at the helicopter rotor by the ground effect.

(a) When the blade pitch angle is big, stalling sometimes occurs when the rotor approaches the ground, and the ground effect causes the increase in the thrust to saturate.

(b) When the blade pitch angle is small, the up-wash from the ground causes a phenomenon similar to autorotation. The torque necessary to maintain the revolution of the rotor increases at first as the rotor approaches the ground, and then it decreases as the up-wash becomes stronger.

(c) In the distribution of the rotor down-wash, the position where the wind velocity is the largest moves toward the circumference as the rotor approaches the ground.

(d) The region where the air flow is stagnant because of the down-wash from the rotor and the up-wash from the ground moves with a certain periodicity.

7. Postscript

It is not necessarily [illegible] pilot to keep the helicopter hovering in the ground effect; they say it feels slippery as if they were on

something like an ice wall. In fact, a large part of helicopter control training is dedicated to hovering, and it is not too much to say that the training starts with hovering and ends with hovering. As we obtained analytical data on the unstable phenomena which seems to be caused by the irregular movement of the down-wash and up-wash, we want to promote a quantitative model on the effects of size, corkscrewing, solidity, position of the rotor, and body type and on the interference at the fixed wing of the compound helicopter developed recently, as well as flight experiments.

Finally, we want to thank the members of the Airplane Body Department who assisted us on numerous occasions when we used the airplane structure laboratory.

We also want to add that these experiments were conducted with the cooperation of the technical officials, Kenji Yazawa, Yukio Kamata, and Yukichi Tsukano.

BIBLIOGRAPHY

1. Gessow, Alfred, and Meyers, Gary C., Jr., Aerodynamics of the Helicopter, The Macmillan Co., c., 1952, pp 106-114.

2. Fradenburgh, Evan A., The Helicopter as a Ground Effect Machine, Sikorsky Aircraft Div., United Aircraft Corp., 1959.

3. Zbrozek, J., Ground Effect on the Lifting Rotor, R. & M. No. 2347, British A. R. C., 1957.

4. Heyson, Harry H., An Evaluation of Linearized Vortex Theory as Applied to Single and Multiple Rotors Hovering In and Out of Ground Effect, NASA TN-43, 1959.

Table 1

Rotor diameter (D)	1100 mm
Chord length of blade wing (c)	33 mm
Blade wing shape	NACA 0012
Downbend of blade (from hub's center)	8°20'
Flapping hinge position	0.0327R = 18 mm
Lugging hinge position	0.0327R = 18 mm
Solidity (σ)	0.0573
Blade weight	109 gram

Table 2

θ_0	0°	5°	10°	15°	20°
$\theta_{0.75}$ (approx)	−5°	0°	5°	10°	15°
$C_{T\infty}$	−0.0023	−0.0001	0.0028	0.0060	0.0069
$C_{T\infty}/\sigma$	−0.0401	−0.0017	0.0489	0.1047	0.1204

Remark: In these experiments, was established at the base of the blade (0.15R), and shows the value at 75% of the length of the blade wing surface.

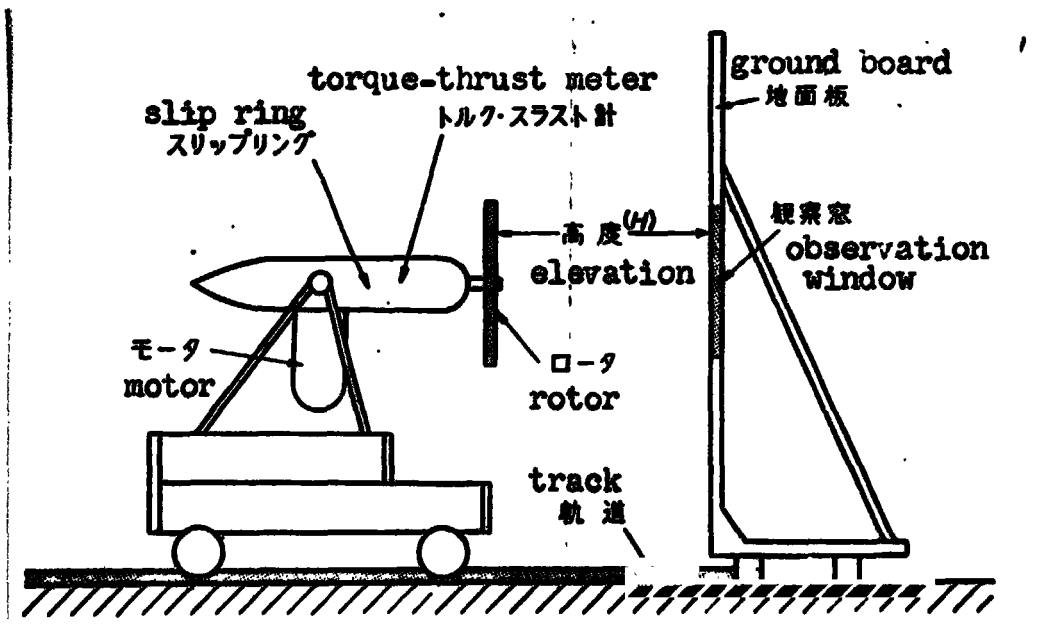

Figure 1 Outline of experimental apparatus

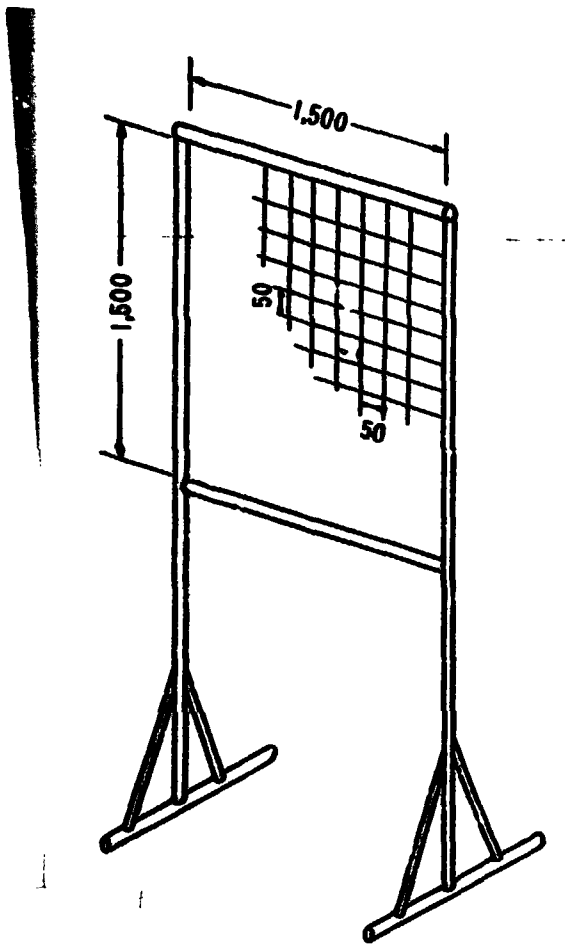

Figure 2 Air flo.: observation net

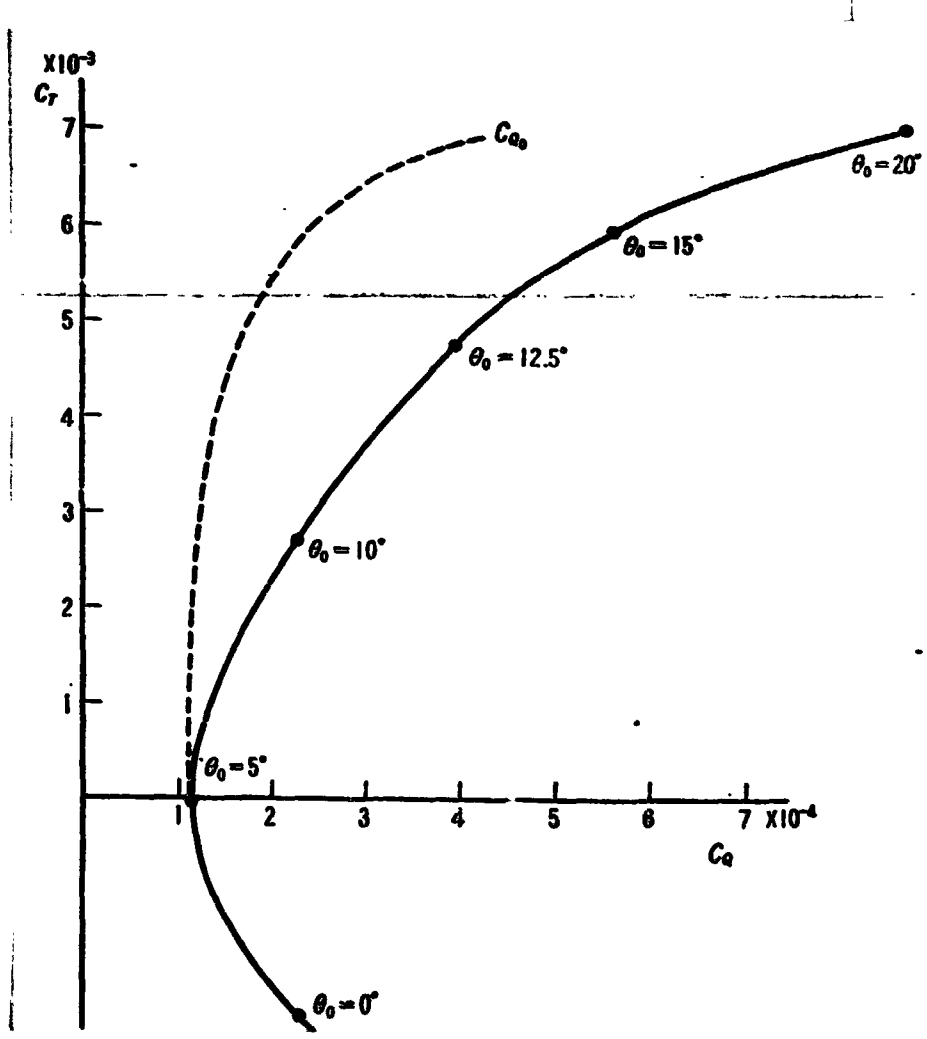

Figure 3
C_T-C_Q curve

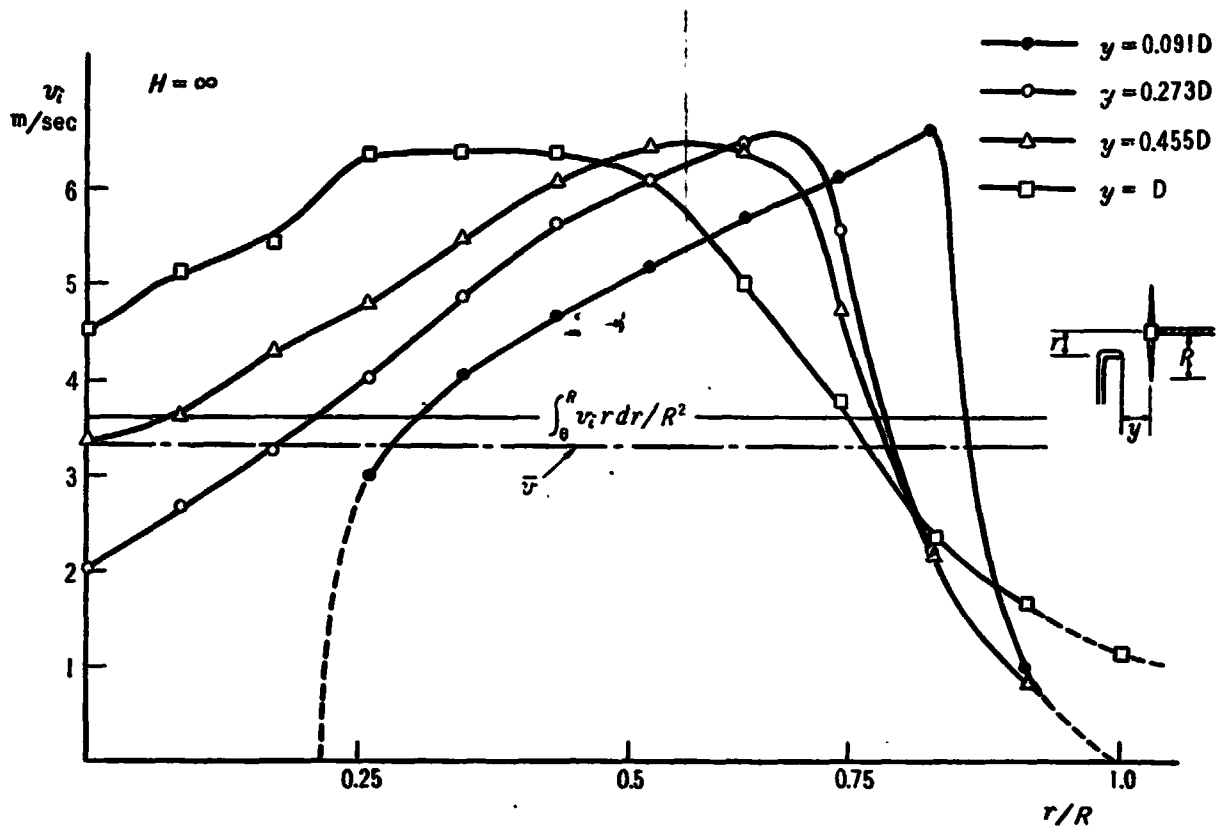

Figure 4 Distribution of induced velocities

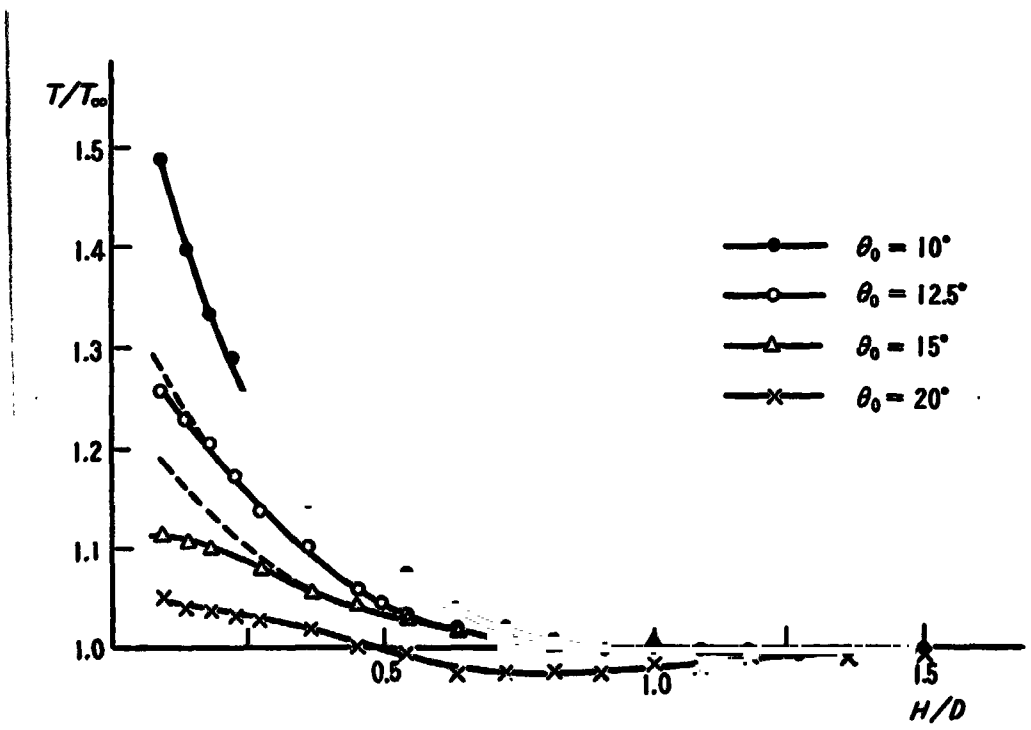

Figure 5 Variation in thrust due to ground effect

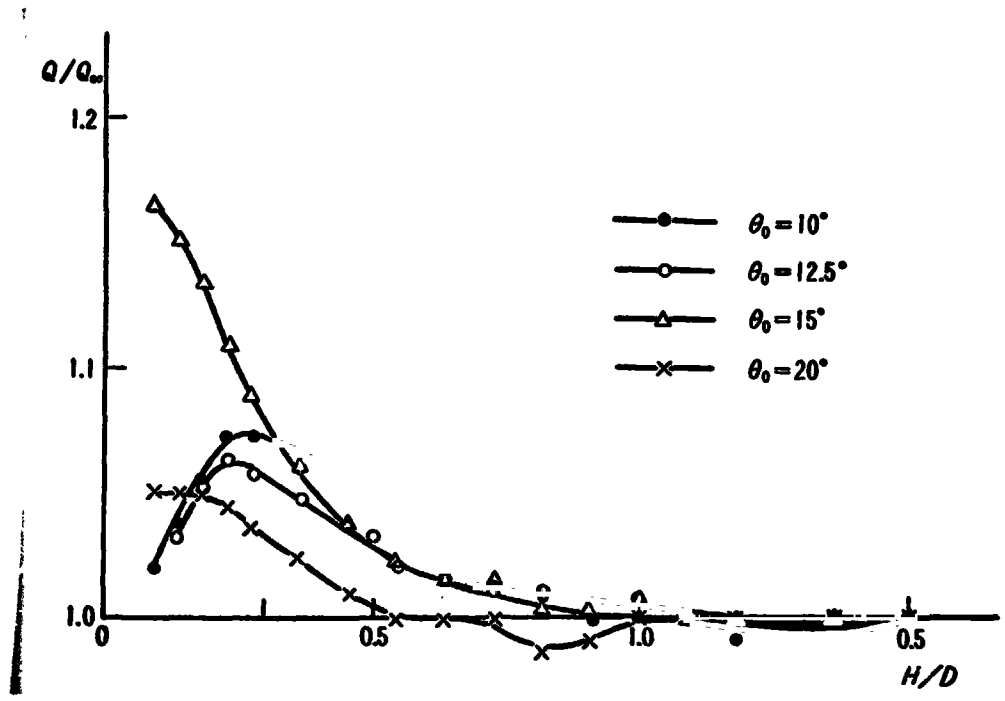

Figure 6 Variation in torque due to ground effect

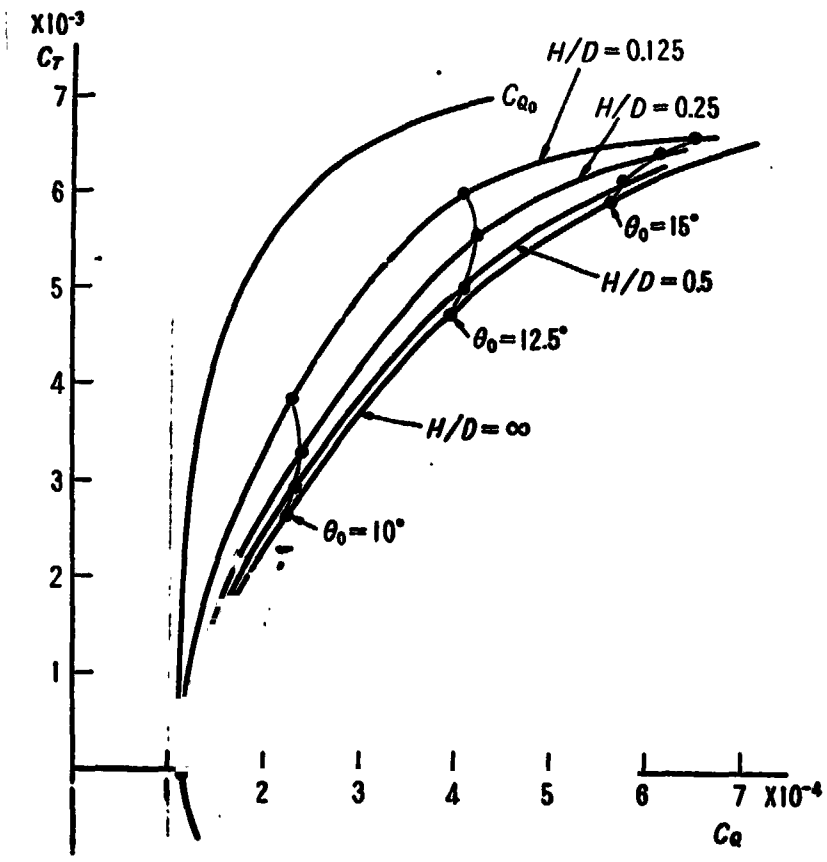

Figure 7 Variation in the C_T-C_Q curve due to ground effect

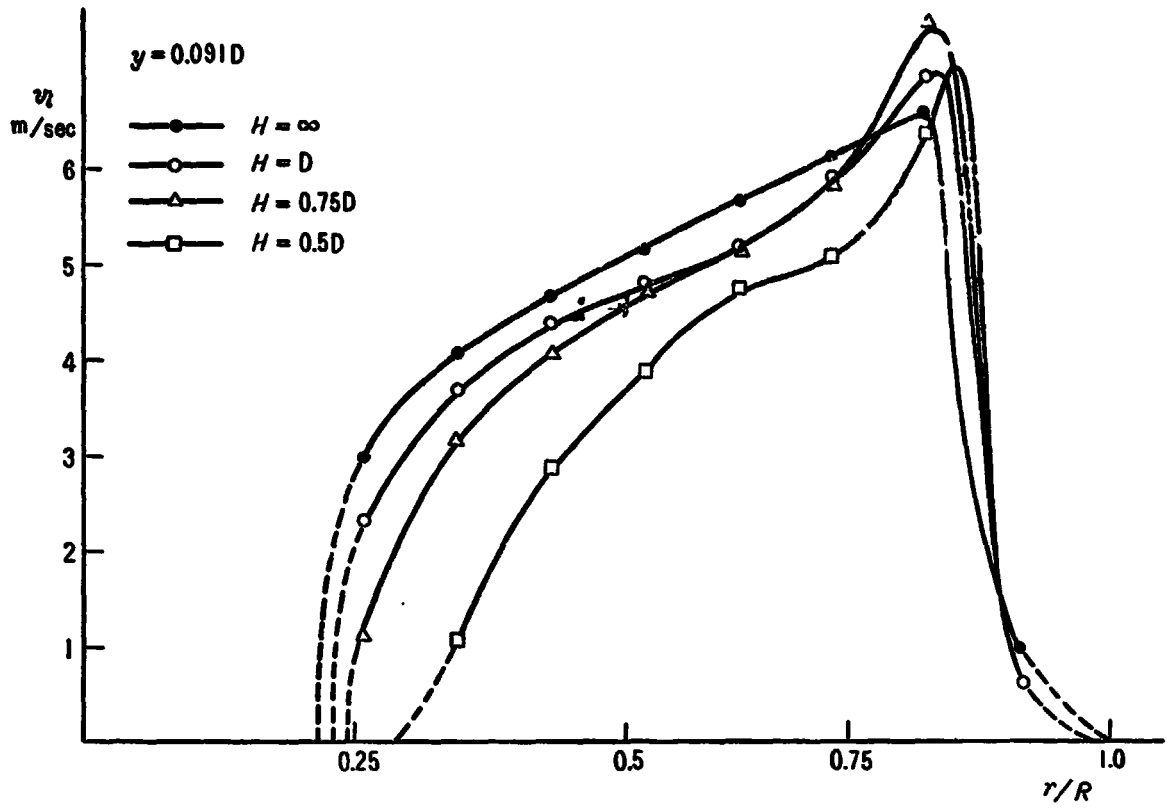

Figure 8 Variation in induced velocity due to ground effect (1)

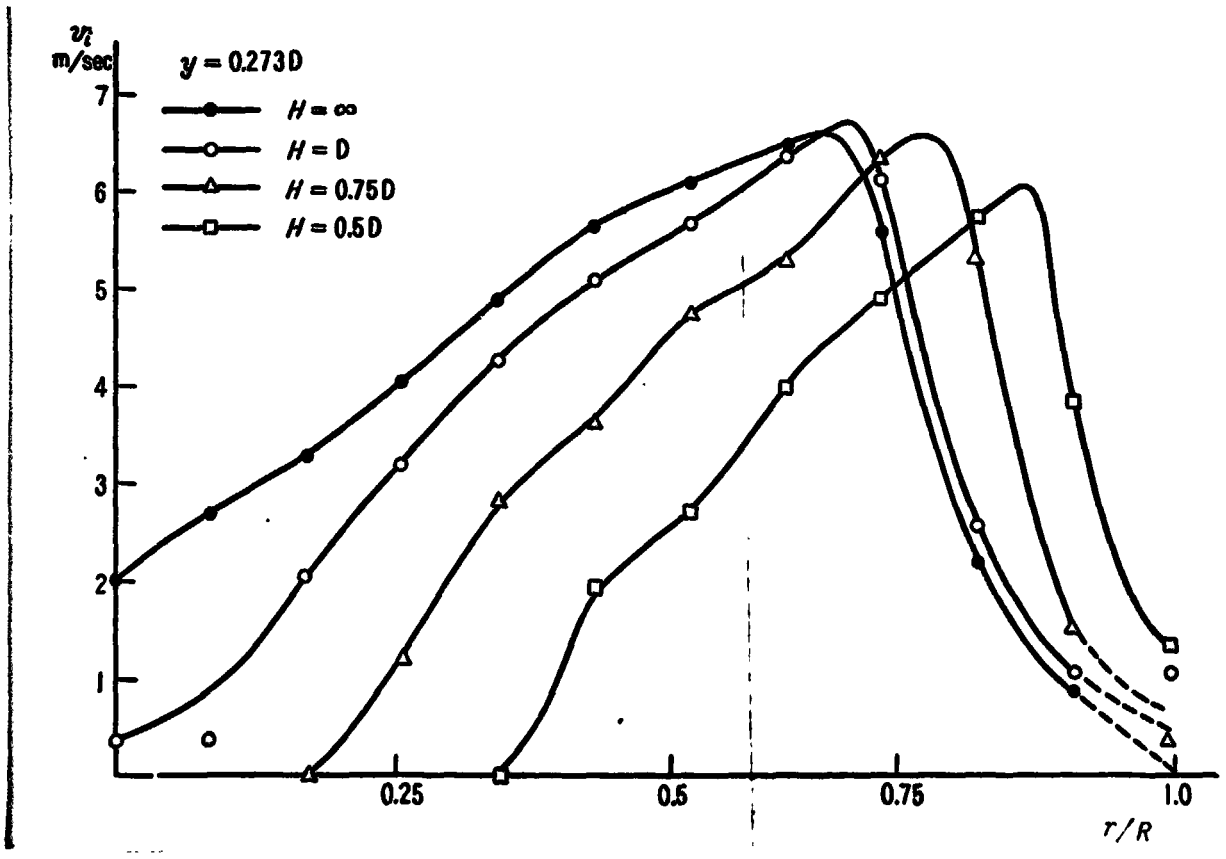

Figure 9 Variation in induced velocity due to ground effect (2)

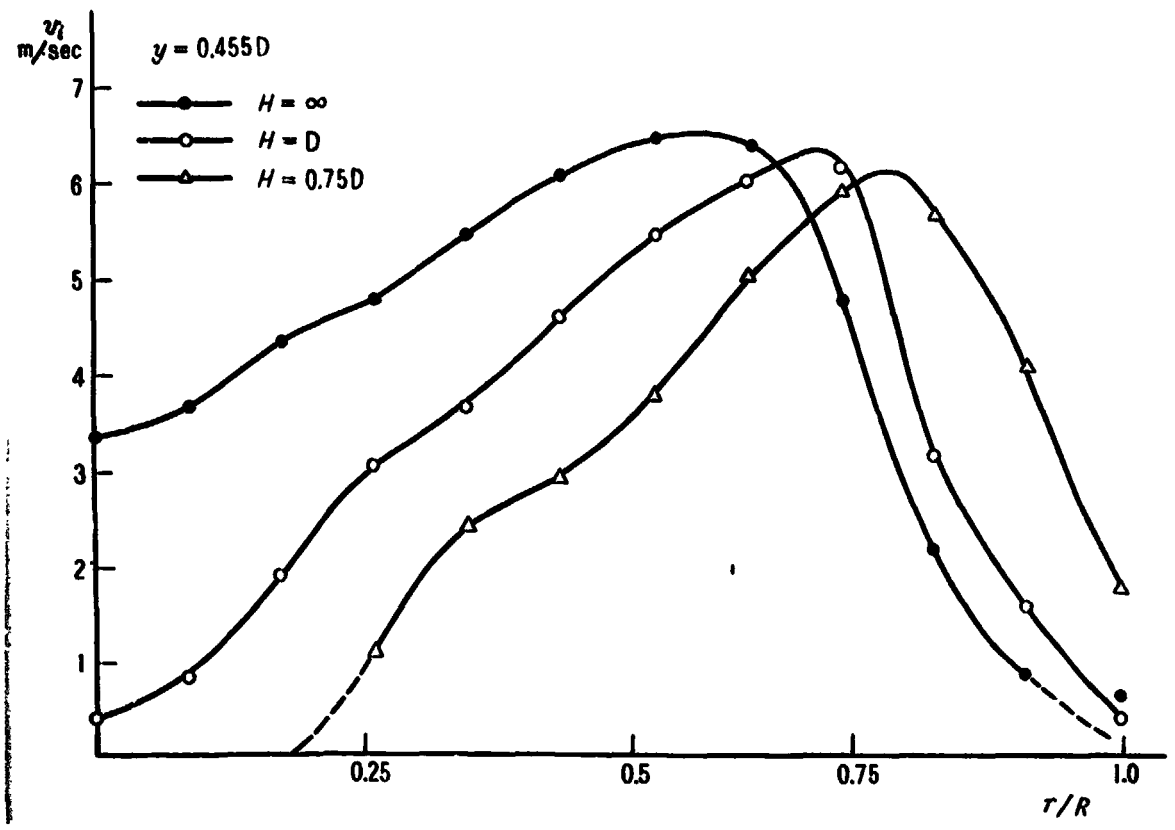

Figure 10 Variation in induced velocity due to ground effect (3)

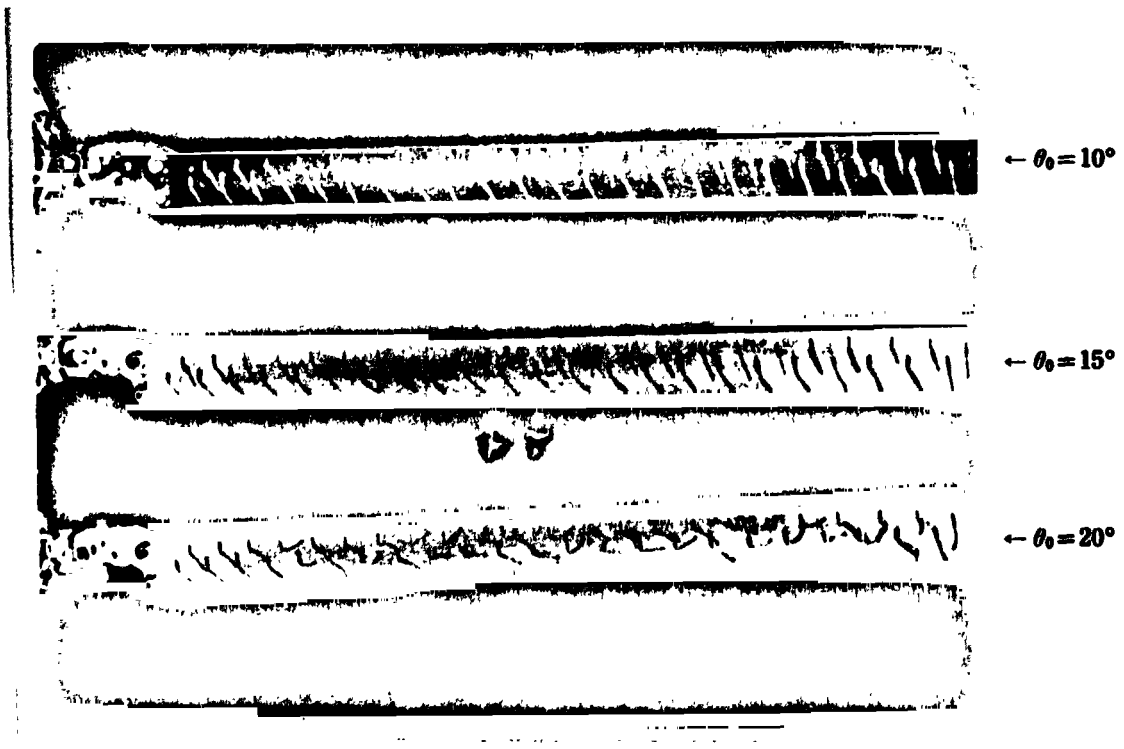

Figure 11 Air flow conditions depending on pitch angle

Figure 12 Variations in air flow on the upper surface of the blade due to approaching the ground (I) (θ_0=15°)

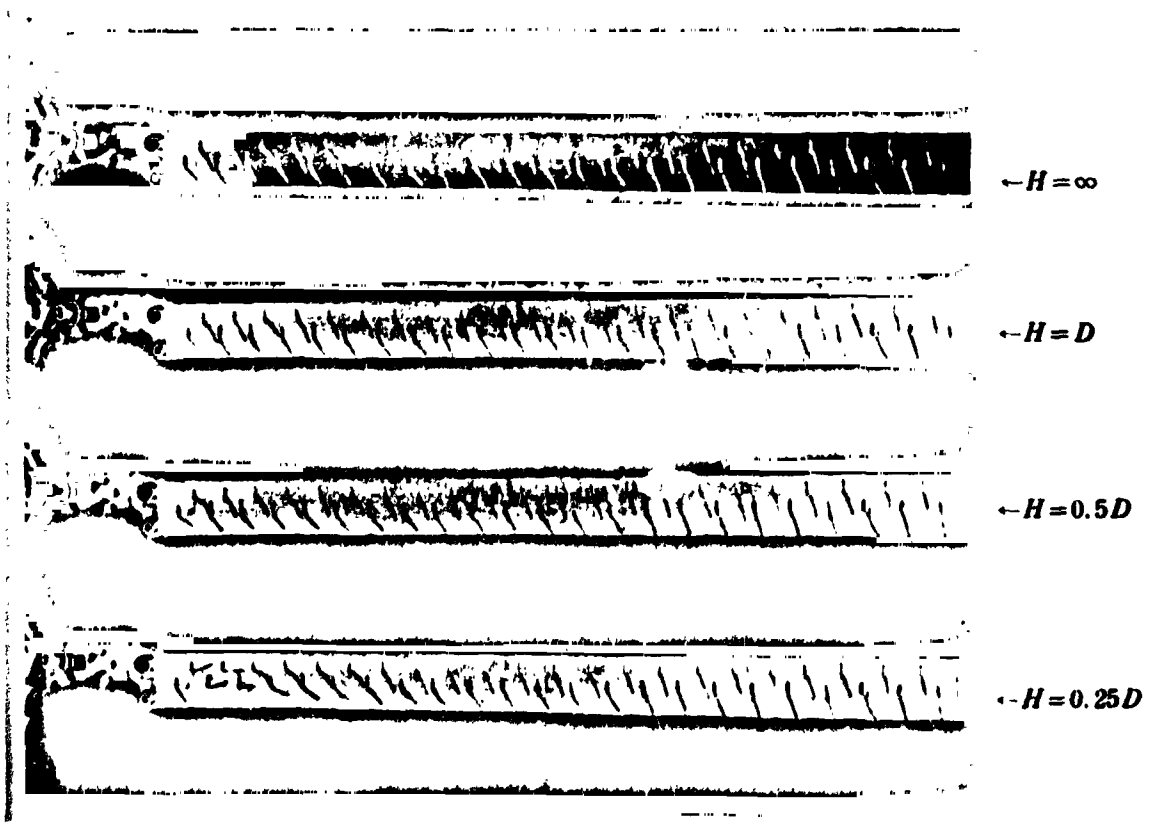

Figure 13 Variations in air flow on the upper surface of the blade due to approaching the ground (II) (θ_0=10°)

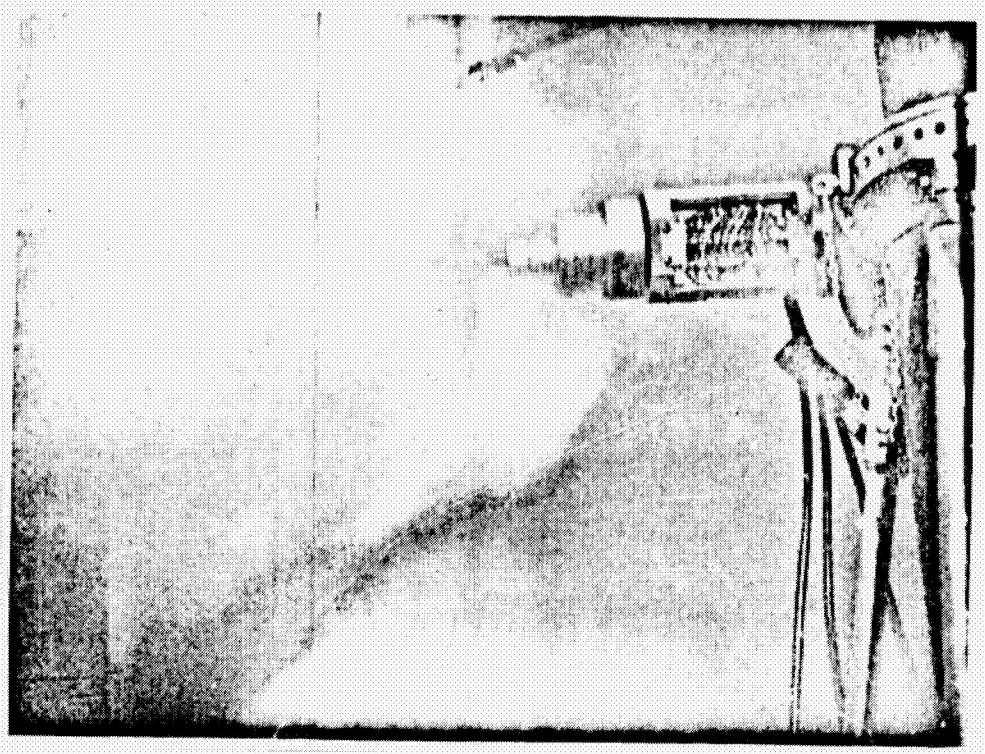

Figure 14 Observation of air flow using smoke (H/D = 0.5)

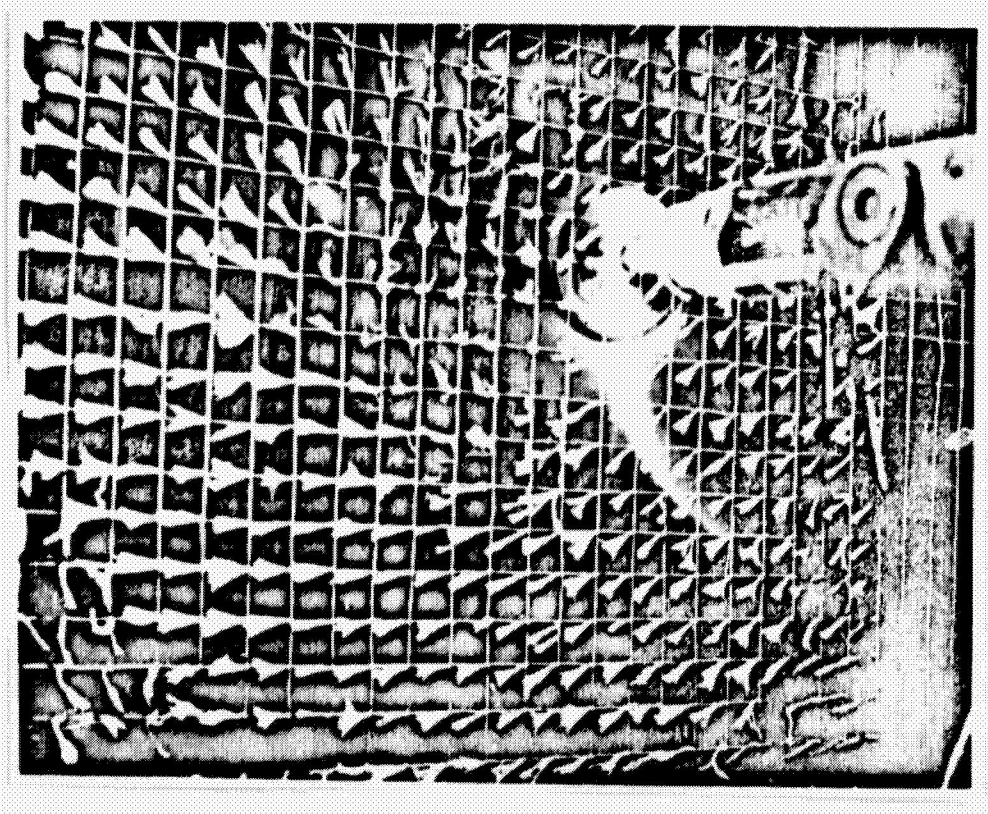

Figure 15 Tufts placed under surface of rotor (H/D = 0.5)

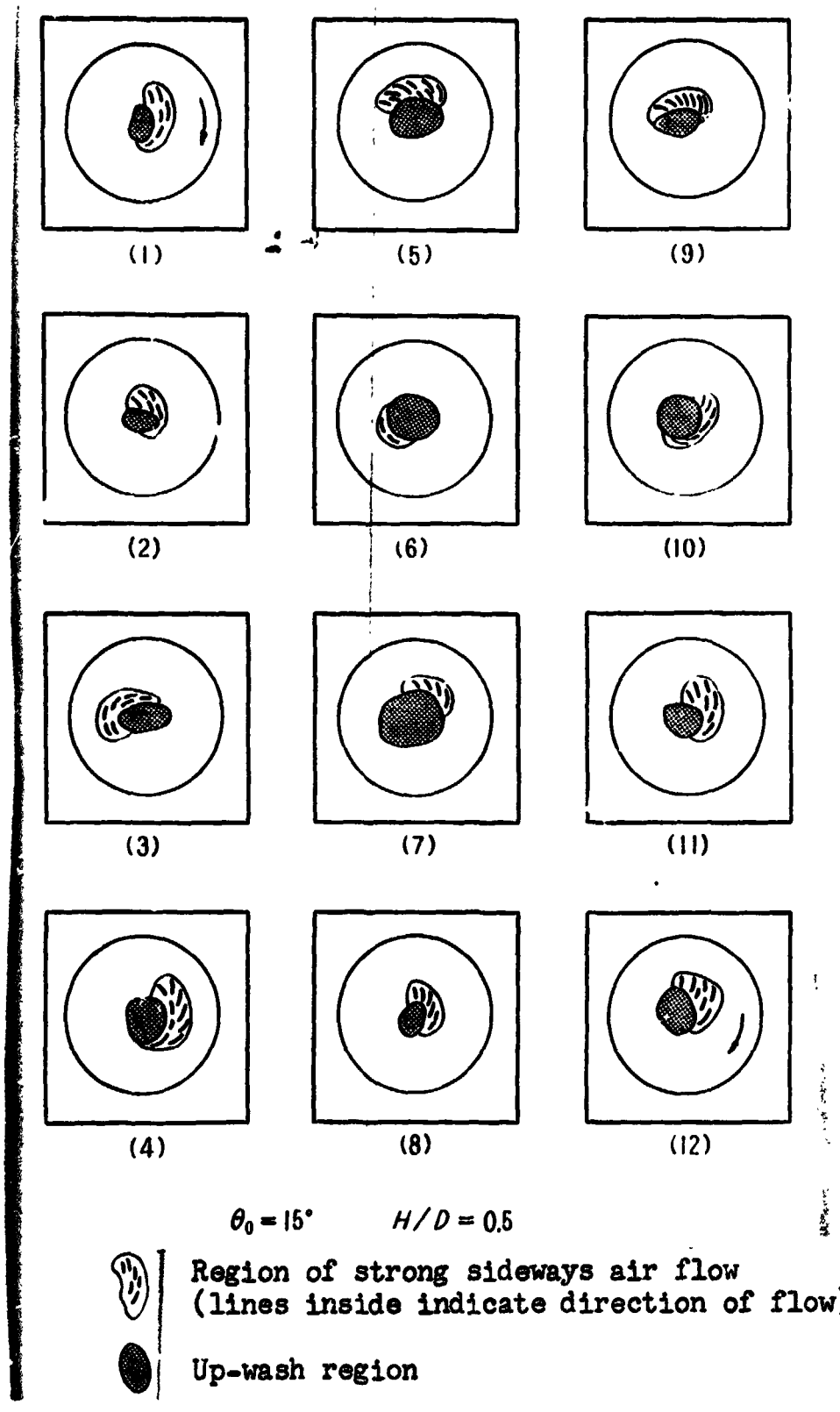

(Sequence of numbers shows changes at 0.5 second intervals)

Figure 16 Variations with time in the direction of air flow under the rotor

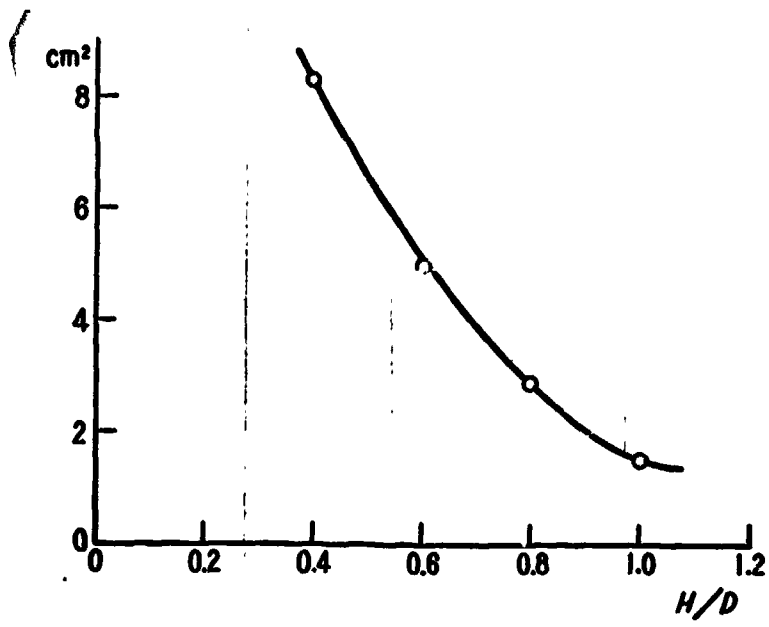

Figure 17 Area of movement of control stick and hovering elevation

- End -